Defect-induced magnetism: Test of dilute magnetism in Fe-doped hexagonal $BaTiO_3$ single crystals

Tanushree Chakraborty
Centre for Advanced Materials, Indian Association for the Cultivation of Science, Jadavpur, Kolkata 700032, India

Sugata Ray*
Centre for Advanced Materials, Indian Association for the Cultivation of Science, Jadavpur, Kolkata 700032, India and
Department of Materials Science, Indian Association for the Cultivation of Science, Jadavpur, Kolkata 700032, India

Mitsuru Itoh
Materials and Structures Laboratory, Tokyo Institute of Technology, 4259 Nagatsuta, Midori-ku, Yokohama 226-8503, Japan
(Received 1 February 2010; revised manuscript received 29 January 2011; published 7 April 2011)

Single crystalline Fe-doped hexagonal $BaTiO_3$ samples with varying oxygen content are created by specifically intended post-growth annealing treatments, in order to check the influence of defects on the unusual high temperature ferromagnetism observed in this system. The various defects have been shown to play a crucial role in dilute magnetic systems and therefore, it is important to carry out this check for the Fe-doped $BaTiO_3$ system also, in which unusual ferromagnetism was reported even in its bulk single crystalline form. The x-ray diffraction and dielectric studies carried out here have confirmed that the Fe doping of Ti is intrinsic, while the high resolution transmission electron microscopy (HRTEM) and x-ray photoemission spectroscopy (XPS) studies proved the absence of unwanted magnetic metal clusters in the sample. The transport studies show that the oxygen concentrations could be varied substantially by the thermal treatments. Finally, magnetization measurements on the samples demonstrated that ferromagnetism is stronger in samples with higher oxygen deficiency, which could interestingly be retreated under high oxygen atmosphere and reversibly be taken back to a lower magnetic state. The vacancy-induced ferromagnetism is further confirmed by EPR measurements, which is consistent with earlier studies and, consequently, put the doped $BaTiO_3$ in the list of true dilute magnetic oxide (DMO) systems.

DOI: 10.1103/PhysRevB.83.144407 PACS number(s): 75.50.Dd, 72.80.Ga, 79.60.Bm

I. INTRODUCTION

Dilute magnetism, i.e., the development of ferromagnetic order with high Curie temperature (T_c) in nonmagnetic semiconducting/insulating materials by the incorporation of only few atomic percent of magnetic impurities, is attracting enormous attention in recent times due to their immense potential in semiconductor based technologies as well as for the growing understanding of new and exciting basic physics. In last few years, dilute magnetic oxides (DMO) have emerged as promising semiconducting/insulating materials they have been reported to exhibit ferromagnetic behavior near or above room temperature,[1–7] although the origin of ferromagnetism in these systems has not been understood and remains controversial till now. Previously, numerous studies on one of the most famous dilute magnetic nonoxide systems, (Ga,Mn)As, have shown that various energetically metastable defects strongly influence the charge carrier density, amount of compensation and consequently, the magnetic parameters like T_c or magnetic susceptibility.[8,9] Consistent with this finding, oxygen vacancies have also been predicted to play a crucial role in modifying or even inducing ferromagnetism in dilute magnetic oxide systems in recent times.[7,10–15] In fact, ferromagnetism has been reported to be an intrinsic property of a number of undoped insulating oxide systems, and is proposed to originate from defect-driven mechanisms only.[16–19] The term d^0 ferromagnetism was suggested to cover these cases.[20,21] Within this defect-driven magnetism, electrons trapped in oxygen vacancy sites (so-called F centers) in DMOs with oxygen deficiencies, have been suggested to be the most essential ingredient to mediate the magnetic coupling,[10] and consistent with this prediction, increasing population of oxygen vacancies have been found to enhance ferromagnetism in many dilute-doped materials. Theoretically, a universal magnetic phase diagram for doped oxides within dilute limit were constructed and it was demonstrated that different magnetic phases may appear in same material depending on the density of oxygen vacancy as well as the concentration of magnetic dopant ions.[10] Therefore, the complete understanding of the ferromagnetic behavior of any dilute magnetic system demands a deeper insight into the complex defect physics, which may eventually lead the way for creating better and novel materials for new applications.

It is extremely important to note here that parallel to this, a large body of research also continues to pose strong questions about the nature of ferromagnetism in such dilute magnetic oxides by simply pointing pointing out various possibilities of extrinsic magnetism, such as dopant clustering, precipitation of impurity magnetic phases, etc., that might occur during synthesis and can possibly be responsible for such unexpected magnetic signals. One strong reason for such doubts is the fact that the equilibrium solubility of the magnetic ions in all the commonly discussed semiconductor/insulator oxides are invariably low, which enforced the usage of improved thin film technologies where synthesis is carried out in conditions far from thermal equilibrium, enabling doping of magnetic ions in concentrations higher than the corresponding thermodynamic equilibrium solubility limits. Such doubts have indeed been substantiated experimentally[22] in the case of at least some

samples, synthesized under certain growth conditions. As a consequence, the search for new host matrices with high equilibrium solubility of impurity magnetic ions has gained momentum in recent years because a successful investigation in this area may not only reduce the uncertainties about secondary impurity phase formation during synthesis but also should encourage further studies with the bulk form of materials, outside the limited thin film regime. Recently, we have proposed a new system,[23] which is possibly the most suitable candidate known till date, in this regard. Hexagonal $BaTiO_3$ is a system known to accommodate a very large amount of transition metal ions replacing Ti^{4+} in the host matrix[24] and we have shown that high temperature ferromagnetism indeed appears in single crystalline $BaTi_{1-x}Fe_xO_3$ with $x < 0.1$,[23] while homogeneously doped ground states with x even up to 0.84 can be stabilized according to the equilibrium phase diagram of this alloy system.[24–26] Based on a detailed first-principle calculation, the magnetic structure of this system was also explained and it was clearly demonstrated that lightly Fe-doped hexagonal $BaTiO_3$ can indeed possess high temperature ferromagnetism although as a whole all possible magnetic interactions may accompany this aspired ferromagnetism, depending on different stabilization conditions.[23] Now, it is expected that oxygen vacancy defects should play a critical role here too because all the current understanding of ferromagnetism in DMOs' categorically states so. Therefore, a deeper understanding of this system would require knowledge about the possible effect of oxygen vacancies on the observed ferromagnetism, and such a study should also provide us a handle to suitably achieve widely different magnetic ground states for the same material by marginally varying experimental conditions.

In this paper, we report detailed magnetic and other physical property studies on three single crystalline samples of 5% Fe-doped hexagonal $BaTiO_3$, possessing grossly different oxygen stoichiometry. All the experimental results, presented here, unarguably establish Fe-doped $BaTiO_3$ as a true member of DMO (dilute magnetic oxide) family and consequently take us one step closer to a complete understanding of this unusual magnetic phenomenon.

II. EXPERIMENTAL DETAILS

Conventional floating zone technique has been employed to synthesize large single crystals of 5% Fe-doped hexagonal $BaTiO_3$. Firstly, dense ceramic rods of nominal composition were prepared by conventional solid state synthesis. Stoichiometric amounts of $BaCO_3$, TiO_2, and Fe_2O_3 were weighed and then thoroughly mixed in agate mortar with ethanol and the resultant powder was then pressed under hydrostatic pressure to obtain rods of suitable dimensions, which were then calcined at 1400 °C in air for 6 h. These hard rods of high material density were used as seed and feed rods for single crystal growth in the floating zone furnace equipped with 1500 W power lamp. Crystal growth was carried out in flowing Ar gas with a growth rate of 7 mm/hr. Seed and feed rods were counter-rotated at 42 r.p.m. An uncontrolled diffusion process during the high temperature containerless growth of a single crystal often leads to significant loss of oxygen,[27] affecting the physical properties of the grown material rather severely and therefore, post-growth annealing in O_2 atmosphere is commonly employed as an attempt to compensate for such extrinsic defects. Accordingly, a ∼1 mm thick piece was cut from the as-grown single crystal rod of an approximate 5 mm diameter, using a diamond cutter, and annealed in oxygen atmosphere at 1000 °C for a period of 12 h. This sample will be mentioned as OFBTO05 in the text from now onwards. Next, two nearly identical pieces were cut from the same as-grown crystal and were annealed at the same temperature and duration inside an evacuated quartz tube in presence of Ti metal (acting as oxygen getter), where the physical separation between them (sample and Ti metal) throughout the annealing process was carefully ensured. The range of vacuum were intentionally kept different for the two pieces. The sample annealed under $\sim 10^{-2}$ mbar pressure is expected to be mildly oxygen deficient and will be termed as RFBTO05**M**, while the piece annealed under $\sim 10^{-5}$ mbar pressure would certainly possess larger amount of oxygen vacancy and will consequently be called RFBTO05**L**. It is to be noted here that the only difference between these samples was the chemical environments (oxidizing or reducing) for the annealing treatments while every other parameters were deliberately kept the same.

Powder x-ray diffraction (XRD) measurements were carried out in a Bruker D8 Advance X-Ray Diffractometer using CuK_α radiation. The diffraction data were analyzed using the Rietveld method and the refinement of crystal structure was carried out using the FULLPROF software.[28] The ac conductance (G vs T) and dielectric (ϵ' vs T) measurements were carried out inside a commercial quantum design physical property measurement system (PPMS) using a LCR meter, spanning a frequency range between 50 Hz to 1 MHz. The transmission electron microscopic (TEM) measurements were carried out in a JEOL2010 microscope. The dc magnetization measurements were carried out in a quantum design SQUID magnetometer both as a function of temperature and as a function of magnetic field, ranging up to 5 Tesla. The EPR spectra were recorded at 77 K using a JEOL JES-FA200 ESR spectrometer operating at 9.2 GHz. The core level electron spectroscopic studies were performed in a commercial spectrometer from VSW Scientific Instruments Ltd., United Kingdom, equipped with a monochromatized Al $K\alpha$ photon source for x-ray photoemission spectroscopy (XPS).

III. RESULTS AND DISCUSSIONS

In Fig. 1, XRD patterns of OFBTO05, RFBTO05M, and RFBTO05L along with the Bragg reflections from pure hexagonal $BaTiO_3$ are shown. The calculated XRD spectra are laid over the experimental data points as solid lines. Evidently, XRD patterns from all the three samples appear very similar and match well with the pattern of hexagonal $BaTiO_3$, while no traces of any other impurity phases were observed. Overall, these experiments provide preliminary indication that post-growth annealing processes under different annealing environments (oxidizing and reducing) do not facilitate any secondary phase formation, at least down to the detection limit of x-ray diffraction. Therefore, the next important issue would be to probe the samples by different techniques and to seek

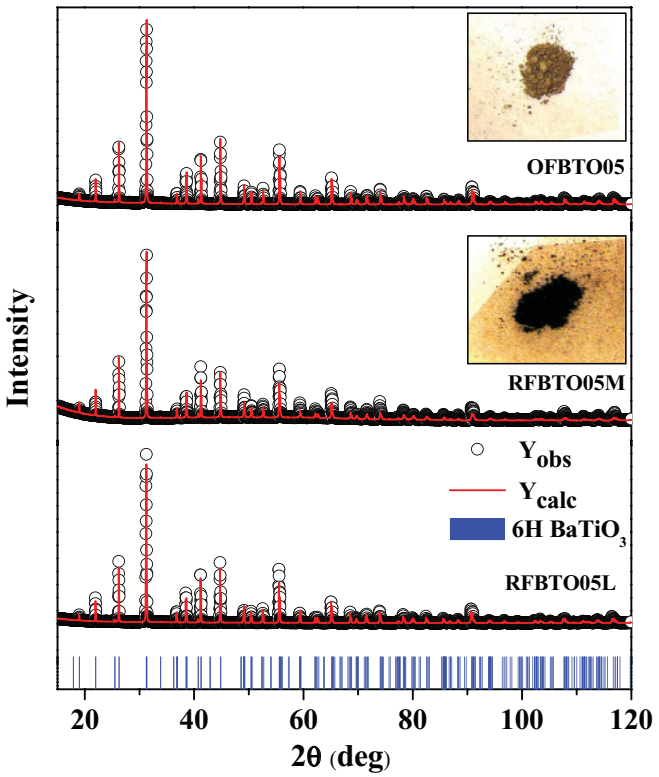

FIG. 1. (Color online) (a) Powder XRD from the OFBTO05, RFBTO05M, and RFBTO05L samples (open circles) along with the Bragg reflections of a pure hexagonal $BaTiO_3$ sample. The refined diffraction spectra are shown on the data as solid lines. The physical appearance of the corresponding powders are shown as insets.

whether there is any effect at all of these different post-growth treatments, given to the single crystalline FBTO05. According to our initial expectation, the RFBTO05M and RFBTO05L sample should contain much larger concentrations of oxygen vacancies, which should consequently influence many physical parameters like electrical conductivity and even the color of the material. Oxygen vacancies are expected to act as double electron donors in the system and therefore, an enhancement in charge carrier (electron here) density in the oxygen deficient sample should enhance electrical conductivity, even if some of the carriers remain trapped in the vacancy sites (F centers). Increased carrier density can also give rise to changes in optical transitions, resulting changes in material colors. In Fig. 1, images of OFBTO05 and RFBTO05M powders are shown. The dense pieces of crystals were all dark in color even after the post-growth annealing treatments but showed very different colors when ground to powder forms. Consistent with our expectations, the RFBTO05M (also RFBTO05L, not shown here) appear almost black while the OFBTO05 sample was dark yellow in its powdered form, indicating different optical transition energies, depending on different concentrations of charge carriers.

In Fig. 2, more quantitative results are summarized, which further support our idea of varying the charge carrier density in the samples by means of different thermal treatments. In panel (a), three characteristic XRD peaks (3 2 4 and 1 1 12) of the same hexagonal $BaTiO_3$ structure, but from three different samples with different oxygen contents, are shown. The instrumental shifts were corrected using a Si internal standard. Evidently, there is a substantial increase in the corresponding d values for the RFBTO05M and further in RFBTO05L sample compared with the OFBTO05 sample, which marks an extension of lattice with increasing oxygen vacancy. The lattice parameters of these samples determined from the Rietveld refinements of the XRD patterns are shown in Fig. 2(b). It is observed that the lattice parameters, and accordingly, the total lattice volume increases substantially by the extraction of oxygen anions from the host matrix. This effect is consistent with previous reports for pure and Fe-doped $BaTiO_3$[29,30] and can be easily explained by the increasing Coulomb repulsion that might arise between the cations in absence of intervening charge compensating anions. We have also estimated the oxygen stoichiometry from the refinements of the samples and it was observed that the RFBTO05L sample possess a large oxygen deficiency ($BaTi_{0.95}Fe_{0.05}O_{2.95}$), while there is no substantial oxygen vacancy in OFBTO05. Due to the poorer data quality, the oxygen stoichiometry in RFBTO05M sample could not be refined satisfactorily though the lattice parameter variation indicates substantial vacancy concentration in this

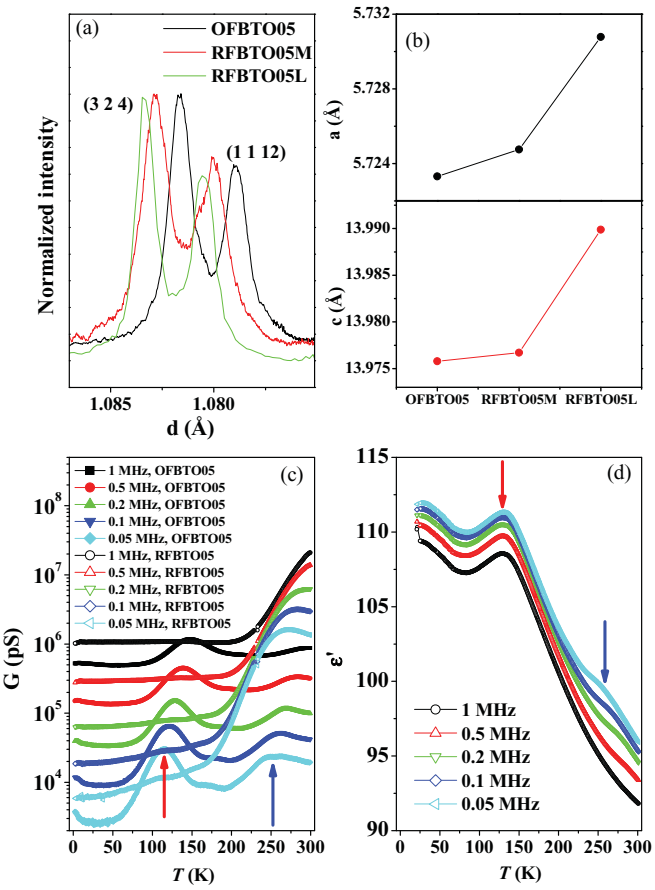

FIG. 2. (Color online) (a) Characteristic XRD peaks from OFBTO05, RFBTO05M, and RFBTO05L samples as a function of d spacing, which indicates clear changes in lattice parameters between the samples. (b) The lattice parameter variations obtained from refinement. Panel (c) shows the ac conductivity data from the two samples, collected with five different frequencies, while the dielectric constant vs T data from the OFBTO05 sample is shown in (d).

sample as well. In panel (c), the ac conductance data from the two samples (OFBTO05 and RFBTO05M) at different frequencies are shown. These measurements were carried out across thin disks of the samples, while the electrical connections were made by sputtering gold on the polished surfaces, followed by sticking Pt wires to the electrodes using Ag paste. A wide frequency range of measurements show that indeed the conductance values of the RFBTO05M sample could be a few orders of magnitude higher than that of the OFBTO05 sample, especially at higher temperatures, indicating higher charge carrier density in the RFBTO05M sample. It is important to note here that both the samples show two characteristic peaks in the conductance curves at around 115 K (red arrows) and 252 K (blue arrows), respectively, and both of them exhibit frequency dispersions. A clear correspondence to these transitions can be observed in the $\epsilon' vs. T$ data of the oxygen annealed 5% Fe-doped $BaTiO_3$ sample [Fig. 2(d)]. Interestingly, the dielectric curve of the 5% Fe-doped $BaTiO_3$ sample is much different from the undoped hexagonal $BaTiO_3$, or even from 1% Fe-doped sample.[23] The $D-E$ loop measurements (not shown here) indicate that ferroelectricity is completely destroyed with Fe doping. This observation very strongly suggests that the Fe ions do replace the Ti ions of the hexagonal $BaTiO_3$ because otherwise such large changes in the dielectric/ferroelectric behavior can not be understood. Overall, the results presented in Fig. 2 establish two important facts about this system. Firstly, the dielectric measurements confirm the substitutional replacement of Ti by Fe and secondly, through the lattice parameter and conductivity changes, the effectiveness of our protocol to vary charge carrier density in these samples, without causing any other perceivable chemical changes is proved.

The high resolution transmission electron microscopy (HRTEM) technique has become a widely used and important tool to study these unusual DMO materials, which is primarily used to search for small magnetic clusters with different crystalline structure parameters within the host matrix that might be invisible to XRD measurements but could provide spurious magnetic signals. HRTEM measurements on the OFBTO05 sample both in powdered form, spread over carbon grids, as well as directly on single crystal plates, thinned to electronic dimension by the use of focused ion beam (FIB) were discussed earlier in Ref. 23. It was shown that no such secondary phase clusters could be detected in OFBTO05 by the HRTEM studies, and only extended, defectless lattice fringes were noticed.[23] In Fig. 3, we show HRTEM images from the RFBTO05M sample only. It is understood that such microscopic studies can never exhaustively cover the whole sample, however, our extended effort did not reveal presence of any secondary phase materials in this sample either. Instead of showing the defect free extended lattice images from this sample, we show few representative images in Fig. 3, that might lead to doubts, but a further careful look failed to establish the presence of secondary phase(s). Clearly, existence of crystal defects as well as Moiré patterns[31,32] could be detected in a few places, as indicated in the figure. Sometimes the contrast variations could be deceiving, while expanded imaging helped to remove doubts, as shown clearly in the lower two panels of Fig. 3. A selected area electron diffraction pattern confirmed good crystallinity of the material.

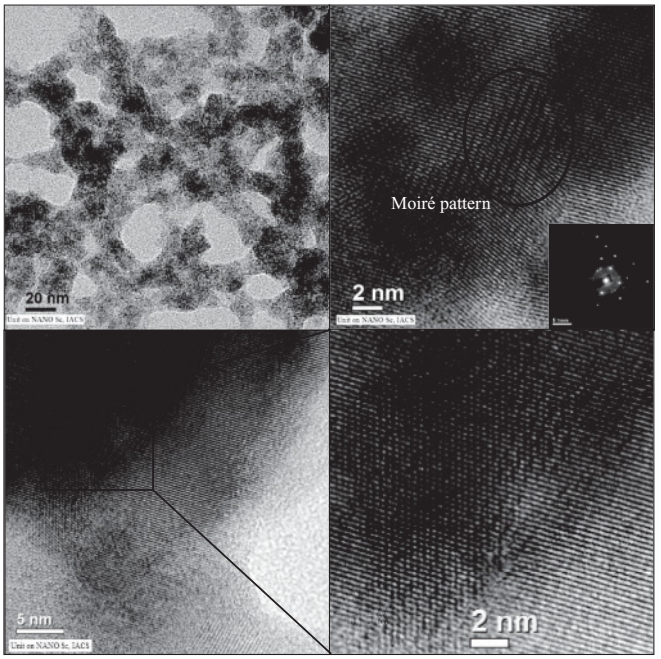

FIG. 3. High resolution TEM images from RFBTO05M sample at room temperature. Different defect structures are indicated.

The different experimental results described above quite clearly establishes the fact that it is possible to incorporate large amounts of oxygen vacancies by simple annealing treatments and without creating any secondary phases or metal clusters. However, the central point of this investigation is to probe whether changing oxygen vacancy does affect the unusual high temperature ferromagnetism or not and if yes, whether the change takes place along the expected line. Therefore, the most crucial experiments are the high quality dc magnetic measurements, which we have carried out and the results are summarized in Fig. 4. Firstly, in Fig. 4(a), we show the temperature dependence of field cooled (FC) and zero field cooled (ZFC) dc magnetic susceptibility (χ) from all the samples, collected with an applied magnetic field of 200 Oe. The overall qualitative behavior appears similar, resembling the mean-field paramagnetic $\chi(T)$ pattern, but none of them truly follow a Curie-Weiss dependence. It is evident from these data that the high temperature magnetic susceptibility got enhanced by more than an order of magnitude in the oxygen deficient samples, compared to the OFBTO05, although the magnetizations at the lowest temperature appear comparable. Therefore, consistent with previous reports, here too, the presence of larger vacancy concentration seems to heighten ferromagnetism in the sample. The somewhat lower susceptibility of RFBTO05L might be an effect of different M-H dependencies at lower fields. However, as the nominal Fe-ion concentration in all the samples remains identical, it can be easily concluded that more number of Fe ions should be interacting ferromagnetically in the more oxygen deficient samples, which might have been behaving like noninteracting paramagnetic spins in the OFBTO05 sample. Earlier it was shown[23] that such doped systems actually represent a soup of inhomogeneity where only a fraction of dopant ions participate in ferromagnetic interaction,

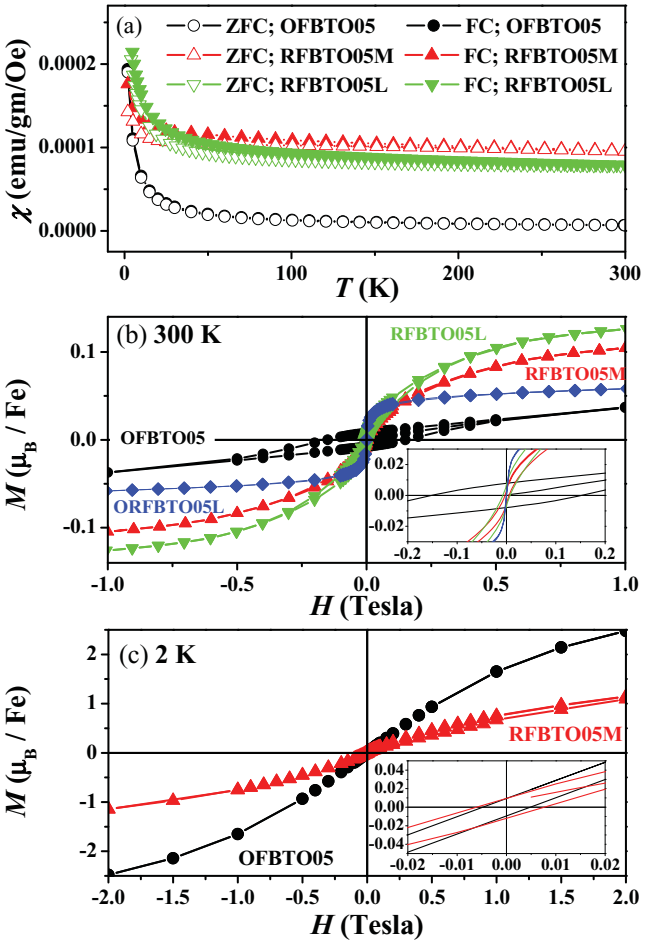

FIG. 4. (Color online) (a) The FC and ZFC magnetic susceptibilities from the OFBTO05 (circles), RFBTO05M (up triangle), RFBTO05L (down triangle) samples are shown in this panel. (b) and (c) display the $M(H)$ curves from the samples at 300 K and 2 K, respectively. The $M(H)$ curve from the ORFBTO05L (diamonds) is also included in panel (b). Insets to (b) and (c) show an expanded version of the same curves that are displayed in the main frame.

while the rest of the dopant ions remain paramagnetic or even antiferromagnetic, depending on their occupancy sites. Therefore, the development of ferromagnetism in RFBTO05M and more so in RFBTO05L sample should come at the expense of these paramagnetic/antiferromagnetic spins.

In the lower panels of Fig. 4, we show the results of magnetization (M) vs applied magnetic field (H) measurements from our samples at room temperature (b) and 2 K (c). Clearly, all the three samples exhibit ferromagnetic behavior at room temperature although significant qualitative as well as quantitative differences are observed between them. Following the expectation, the magnetic moments of the samples at room temperature increase regularly with increasing vacancy concentrations. More importantly, the room temperature $M(H)$ curves of the RFBTO05M and RFBTO05L samples start to exhibit behavior of conventional ferromagnet with small loop structure but clear indications of saturations at higher fields. Interestingly, the 2 K data from the samples (RFBTO05L not shown here) appear qualitatively similar with smaller loop structures but consistent with the susceptibility pattern, the high-field moment from the $M(H)$ curve (resembling more a paramagnetic Brillouin function) is smaller for RFBTO05M. In order to probe whether the influence of oxygen vacancy on the observed ferromagnetism is reversible or not, the RFBTO05L sample was reannealed in oxygen atmosphere at 1400 °C. This sample is named as ORFBTO05L. The room temperature $M(H)$ curve from this sample is displayed in Fig. 4(b), which indicates a drastic reduction in the magnetic moment for this sample. Although, the nature of the $M(H)$ loop could not be retraced (between OFBTO05 and ORFBTO05L), the lower moment definitely establishes the fact that again the amount of ferromagnetically interacting Fe dopants has diminished with reducing concentration of oxygen vacancies. Therefore, the ferromagnetism in the present sample could be manipulated by carefully varying the donor defects, i.e., the oxygen vacancies.

The magnetization measurements clearly indicate that with increasing oxygen vacancy concentrations more and more Fe dopants start to interact magnetically, while the contribution from noninteracting paramagnetic-like Fe spins diminish. In order to further check this point, we have carried out X-band EPR measurements on our samples and the results are summarized in Fig. 5. The hexagonal $BaTiO_3$ is trigonally distorted along the c axis and the degree of distortion is different in the corner-shared and face-shared octahedra (see inset to Fig. 5). It is expected that there will be fluctuations in local lattice parameters in the vicinity of paramagnetic Fe^{3+} ion ($S = 5/2$) and as a result, a distribution of fine structures (FS) are observed in the EPR spectrum. At the top of Fig. 5, we show the EPR spectrum from OFBTO05 sample, which exhibits a number of FS peaks. This spectrum matches extremely well with earlier reports on Fe-doped hexagonal $BaTiO_3$,[33] which confirms that this sample possesses a large concentration of uncorrelated Fe spins. However, the EPR spectrum gets drastically modified with increased oxygen vacancy, where there is only one EPR signal with large peak-to-peak linewidth and enhanced intensity (in the plot, normalized intensities are plotted for the sake of easy visual comparison). Such an EPR signal is invariably reminiscent of strong Fe-Fe magnetic interaction as is observed in many strongly magnetic iron compounds. A representative spectrum from $LaMn_{0.5}Fe_{0.5}O_3$ having transition metal ions in octahedral coordination is shown at the bottom, which has been reproduced from Ref. 34. The striking similarity between the two confirms that indeed the majority Fe spins are interacting ferromagnetically in RFBTO05L, with enhanced oxygen vacancy concentrations, and as a result, nearly saturated $M(H)$ loops with enhanced magnetic moment is observed in RFBTO05L, which was elusive in OFBTO05 [Fig. 4(b)]. Very similar EPR signal was also observed in Fe-doped ZnO dilute magnetic oxide.[35]

We have also attempted to carry out Hall measurements on these single crystal samples in order to investigate the variation of carrier concentrations in them. The Hall measurements were performed in a two-dimensional van der Pauw geometry (see the inset to Fig. 5). However, the high electrical resistance of all the samples and the lack of facility to employ a three-dimensional measurement geometry hindered the measurements and perfect quantitative data

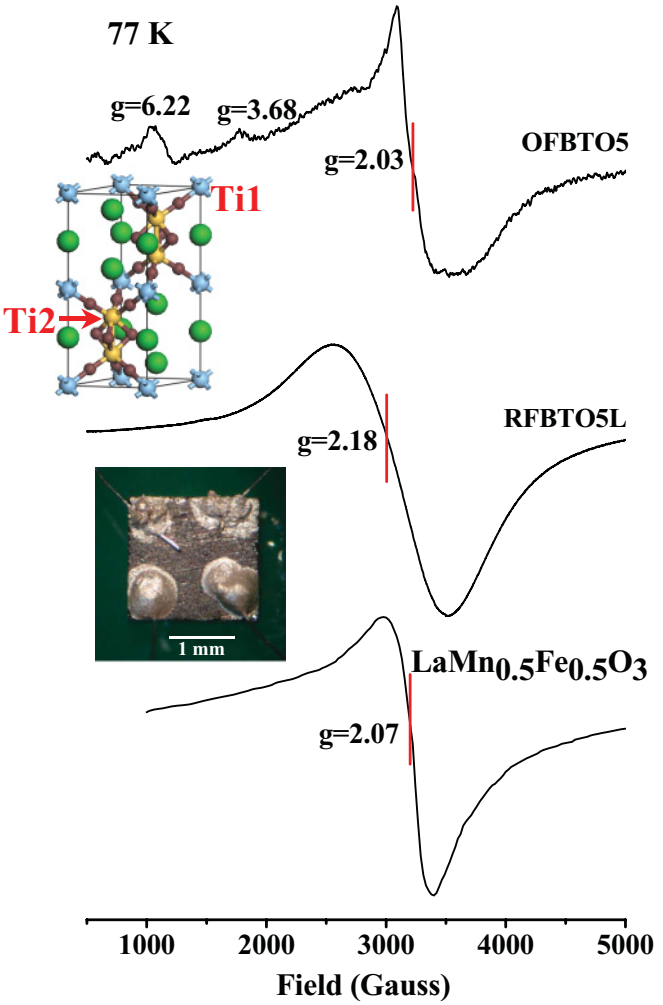

FIG. 5. (Color online) EPR spectra from OFBTO05 and RFBTO05L, collected at 77 K along with the $LaMn_{0.5}Fe_{0.5}O_3$ spectrum reproduced from Ref. 34. Insets show hexagonal $BaTiO_3$ structure and an image of a crystal piece with four probes attached to it for transport measurements.

about the carrier concentration could not be obtained. In Table I, we summarize the dc resistivity values from the samples as well as rough estimates of carrier concentrations, obtained from this setup. The results further confirm the effect of vacancy concentration on the transport property of the material.

We have also carried out core level photoelectron spectroscopy measurements on the RFBTO05M sample, in order to have a consolidated description about the valency and chemical states of the material, especially the transition metals (Ti and Fe). The low concentration of Fe ion in the sample created difficulty in collecting a proper Fe $2p$ spectrum, while

TABLE I. Transport data from the Fe-doped $BaTiO_3$ samples.

Sample	ρ (Ω-cm)	n (cm^{-3})
OFBTO05	2.2×10^6	10^{11}
RFBTO05M	4×10^5	–
RFBTO05L	2.6×10^5	10^{13}

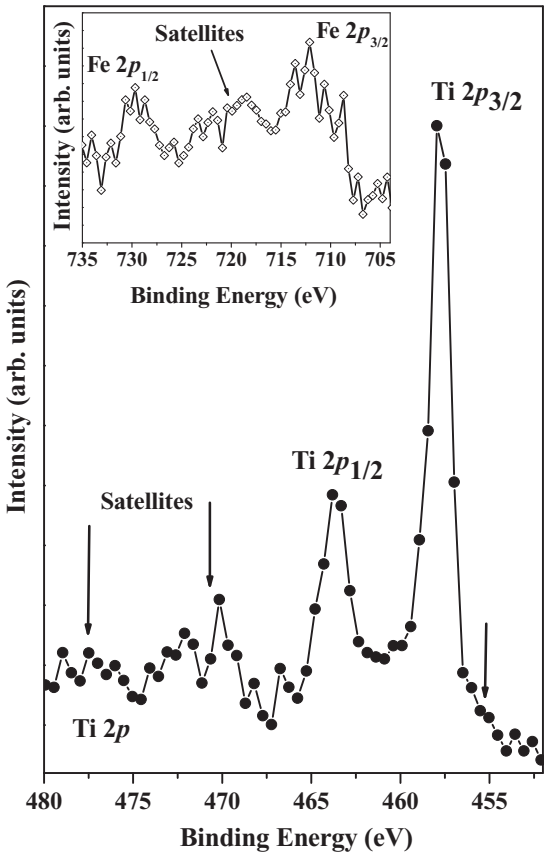

FIG. 6. The Ti $2p$ core level photoemission spectrum from the sample RFBTO05M is shown shown in the main panel, while the inset displays the Fe $2p$ spectrum from the same sample.

the "charging" effect due to the highly insulating nature of sample disturbed the spectral shape as well as the intensity. However, the most important features are shown in Fig. 6. The main panel shows the Ti $2p$ spectrum, where Ti $2p_{3/2}$ and $2p_{1/2}$ peaks appear at 457.8 and 463.6 eV binding energies, with the expected spin-orbit splitting of 5.8 eV for a Ti^{4+} species. Moreover, it is well known that Ti^{4+} oxides, as in $SrTiO_3$[36,37] or TiO_2,[36,38] show weak satellite features, at about 13 eV away from the main peak in the Ti $2p$ spectral region, characteristic of the Ti^{4+} state. In the present case, we can see similar weak satellite features at about 13 eV above the main peaks (marked by arrows). This confirms that majority of Ti is in the formally Ti^{4+} $3d^0$ state in this material. However, a low intensity shoulder at around 455 eV (marked by a down arrow) may indicate presence of little Ti^{3+} species.[39] The Fe $2p$ spectrum is shown in the inset. The binding energy of the peaks and the overall spin-orbit split Fe $2p$ spectrum with accompanying strong satellite features, clearly resemble a Fe^{3+} like spectrum. Most importantly, no lower binding energy features, corresponding to possible Fe-metal clusters are observed. Therefore, the photoemission spectra establish that the description of Fe^{3+} ions replacing Ti^{4+} ions in these materials is the most fitting one.

IV. CONCLUSIONS

In summary, a comprehensive study on the room temperature ferromagnetism has been carried out on the Fe-doped hexagonal $BaTiO_3$ single crystals, grown by floating zone technique. The oxygen content of the sample is varied by employing different post growth annealing treatments. Three samples with varying oxygen contents are studied using XRD, transport, HRTEM, SQUID, EPR, and XPS measurement techniques and the experimental results establish the decisive role of oxygen vacancy on the magnetism of this system. It is observed that the ferromagnetism gets substantially enhanced with increasing oxygen vacancy, which suggests a defect-mediated mechanism. Both the oxygen vacancies and the Fe dopants play critical and complimentary roles to alter the electronic band structure of the host and to modify the long-range ferromagnetic ordering. Furthermore, it is also observed that the vacancy concentration and the related ferromagnetism could be manipulated reversibly. It is to be noted that such dependencies are typical of true dilute magnetic systems, discussed already in case of other systems,[7,10–15,40] and cannot probably be explained in terms of conventional magnetic signals arising from any accompanying spurious impurity phase. It has already been shown[41,42] that presence of several competing magnetic interactions is nearly unavoidable in dilute magnetic systems and different unusual magnetic signals [e.g., highly concave magnetic susceptibility $\chi(T)$] invariably carry signatures of such complicated interactions. In our previous report,[23] we have also shown that the scenario in doped hexagonal $BaTiO_3$ is not very different either and actually offers a vast sea of inhomogeneous magnetic interactions. Here, incorporation of large amount of oxygen vacancies may strongly influence the relative concentrations of differently interacting or noninteracting magnetic species, and consequently, enhance ferromagnetism, as is clearly manifested in this experimental study.

ACKNOWLEDGMENTS

SR acknowledges the Fast Track scheme and the DST-RFBR project by the Department of Science and Technology, Government of India for funding. We thank Dr. T. K. Paine for the help with the EPR measurements, Dr. D. Basak for the help with Hall measurements, and Dr. V. Siruguri for help with refinements. We also thank Dr. D. D. Sarma for providing us the facility to carry out the XPS measurements.

*mssr@iacs.res.in

[1] A. H. MacDonald, P. Schiffer, and N. Samarth, Nat. Mater. **4**, 195 (2005).
[2] Y. Matsumoto, M. Murakami, T. Shono, T. Hasegawa, T. Fukumura, M. Kawasaki, P. Ahmet, T. Chikyow, S. Koshihara, and H. Koinuma, Science **291**, 854 (2001).
[3] K. Ueda, H. Tabata, and T. Kawai, Appl. Phys. Lett. **79**, 988 (2001).
[4] S. B. Ogale, R. J. Choudhary, J. P. Buban, S. E. Lofland, S. R. Shinde, S. N. Kale, V. N. Kulkarni, J. Higgins, C. Lanci, J. R. Simpson, N. D. Browning, S. Das Sarma, H. D. Drew, R. L. Greene, and T. Venkatesan, Phys. Rev. Lett. **91**, 077205 (2003).
[5] J. M. D. Coey, A. P. Doyvalis, C. B. Fitzgerald, and M. Venkatesan, Appl. Phys. Lett. **84**, 1332 (2004).
[6] P. Sharma, A. Gupta, K. V. Rao, F. J. Owens, R. Sharma, R. Ahuja, J. M. O. Guillen, B. Johansson, and G. A. Ghering, Nat. Mater. **2**, 673 (2003).
[7] J. Philip, A. Punnoose, B. I. Kim, K. M. Reddy, S. Layne, J. O. Holmes, B. Satpati, P. R. Leclair, T. S. Santos, and J. S. Moodera, Nat. Mater. **5**, 298 (2006).
[8] T. Hayashi, Y. Hashimoto, S. Katsumoto, and Y. Iye, Appl. Phys. Lett. **78**, 1691 (2001).
[9] S. J. Potashnik, K. C. Ku, S. H. Chun, J. J. Berry, N. Samanth, and P. Schiffer, Appl. Phys. Lett. **79**, 1495 (2001).
[10] J. M. D. Coey, M. Venkatesan, and C. B. Fitzgerald, Nat. Mater. **4**, 173 (2005).
[11] M. H. F. Sluiter, Y. Kawazoe, P. Sharma, A. Inoue, A. R. Raju, C. Rout, and U. V. Waghmare, Phys. Rev. Lett. **94**, 187204 (2005).
[12] G. Z. Xing, J. B. Yi, D. D. Wang, L. Liao, T. Yu, Z. X. Shen, C. H. A. Huan, T. C. Sum, J. Ding, and T. Wu, Phys. Rev. B **79**, 174406 (2009).
[13] L. X. Guan, J. G. Tao, Z. R. Xiao, B. C. Zhao, X. F. Fan, C. H. A. Huan, J. L. Kuo, and L. Wang, Phys. Rev. B **79**, 184412 (2009).
[14] V. Fernandes, R. J. O. Mossanek, P. Schio, J. J. Klein, A. J. A. de Oliveira, W. A. Ortiz, N. Mattoso, J. Varalda, W. H. Schreiner, M. Abbate, and D. H. Mosca, Phys. Rev. B **80**, 035202 (2009).
[15] F.-X. Jiang, X.-H. Xu, J. Zhang, H.-S. Wu, and G. A. Gehring, Appl. Surf. Sci. **255**, 3655 (2009).
[16] Y.-Q. Song, H.-W. Zhang, Q.-Y. Wen, L. Peng, and J. Q. Xiao, J. Phys. Condens. Matter **20**, 255210 (2008).
[17] A. Sundaresan, R. Bhargavi, N. Rangarajan, U. Siddesh, and C. N. R. Rao, Phys. Rev. B **74**, 161306(R) (2006).
[18] Y. Liu, Z. Lockman, A. Aziz, and J. MacManus-Driscoll, J. Phys. Condens. Matter **20**, 165201 (2008).
[19] N. H. Hong, J. Sakai, N. Poirot, and V. Brizé, Phys. Rev. B **73**, 132404 (2006).
[20] J. M. D. Coey, Curr. Op. in Solid State and Mat. Sc. **10**, 83 (2006).
[21] J. M. D. Coey, Solid State Sci. **7**, 660 (2005).
[22] J. Y. Kim, J. H. Park, B. G. Park, H. J. Noh, S. J. Oh, J. S. Yang, D. H. Kim, S. D. Bu, T. W. Noh, H. J. Lin, H. H. Hsieh, and C. T. Chen, Phys. Rev. Lett. **90**, 017401 (2003); A. Punnoose, M. S. Seehra, W. K. Park, and J. S. Moodera, J. Appl. Phys. **93**, 7867 (2003).
[23] S. Ray, P. Mahadevan, S. Mandal, S. R. Krishnakumar, C. S. Kuroda, T. Sasaki, T. Taniyama, and M. Itoh, Phys. Rev. B **77**, 104416 (2008).
[24] T. A. Vanderah, J. M. Loezos, and R. S. Roth, J. Sol. State Chem. **121**, 38 (1996).
[25] I. E. Grey, C. Li, L. M. D. Cranswick, R. S. Roth, and T. A. Vanderah, J. Sol. State Chem. **135**, 312 (1998).
[26] G. M. Keith, M. J. Rampling, K. Sarma, N. Mc. Alford, and D. C. Sinclair, J. Eur. Ceram. Soc. **24**, 1721 (2004).
[27] J. Yu, P. Paradis, T. Ishikawa, S. Yoda, Y. Saita, M. Itoh, and F. Kano, Chem. Mater. **16**, 3973 (2004).
[28] J. Rodríguez-Carvajal, Physica B **192**, 55 (1993).

[29]D. C. Sinclair, J. M. S. Skakle, F. D. Morrison, R. I. Smith, and T. P. Beales, J. Mater. Chem. **9**, 1327 (1999).
[30]I. E. Grey, L. M. D. Cranswick, and C. Li, J. Appl. Cryst. **31**, 692 (1998).
[31]J. Reyes-Gasga, S. Tehuacanero, and M. J. Yacamán, Mic. Res. Tech. **40**, 2 (1998).
[32]M. Klimenkov, S. Nepijko, H. Kuhlenbeck, and H.-J. Freund, Surf. Sc. **385**, 66 (1997).
[33]R. Böttcher, H. T. Langhammer, T. Müller, and H.-P. Abicht, J. Phys. Condens. Matter **20**, 505209 (2008).
[34]S. D. Bhame, V. L. Joseph Joly, and P. A. Joy, Phys. Rev. B **72**, 054426 (2005).
[35]D. Karmakar, S. K. Mandal, R. M. Kadam, P. L. Paulose, A. K. Rajarajan, T. K. Nath, A. K. Das, I. Dasgupta, and G. P. Das, Phys. Rev. B **75**, 144404 (2007).
[36]C. N. R. Rao, D. D. Sarma, S. Vasudevan, and M. S. Hegde, Proc. R. Soc. London A **367**, 239 (1979).
[37]S. Ray, D. D. Sarma, and R. Vijayaraghavan, Phys. Rev. B **73**, 165105 (2006).
[38]A. E. Bocquet, T. Mizokawa, K. Morikawa, A. Fujimori, S. R. Barman, K. Maiti, D. D. Sarma, Y. Tokura, and M. Onoda, Phys. Rev. B **53**, 1161 (1996).
[39]S. M. Mukhopadhyay and T. C. S. Chen, J. Mater. Res. **10**, 1502 (1995).
[40]S. Das Sarma, E. H. Hwang, and A. Kaminski, Phys. Rev. B **67**, 155201 (2003).
[41]M. Berciu and R. N. Bhatt, Phys. Rev. B **69**, 045202 (2004).
[42]A. Kassaian and M. Berciu, Phys. Rev. B **71**, 125203 (2005).